Geomorphology 219 (2014) 248–259

Contents lists available at ScienceDirect

Geomorphology

journal homepage: www.elsevier.com/locate/geomorph

Debris flow activity related to recent climate conditions in the French Alps: A regional investigation

Irina Pavlova [a,*], Vincent Jomelli [a], Daniel Brunstein [a], Delphine Grancher [a], Eric Martin [b], Michel Déqué [c]

[a] Laboratoire de Géographie Physique, LGP/CNRS, 1 place Aristide Briand, 92195 Meudon, France
[b] Météo-France CNRM-GAME/GMME/MOSAYC, 42 Avenue Coriolis, 31057 Toulouse, France
[c] Météo-France CNRM/GMGEC/EAC, 42 Avenue Coriolis, 31057 Toulouse, France

ARTICLE INFO

Article history:
Received 8 June 2012
Received in revised form 10 April 2014
Accepted 17 April 2014
Available online 30 April 2014

Keywords:
Debris flow activity
Climate changes
Intensity/duration thresholds
Logistic regression

ABSTRACT

The primary objective of this study was to document the relationships between current climatic conditions and debris flow activity in the French Alps based on a large historical database of debris flow events covering 35 years up to the present. The French Alps are composed of two contrasting geographic areas so two debris flow regions with different activity patterns were defined. For the period 1970–2005, the database contains 565 debris flow events in 87 catchments in the northern part of the French Alps, and in 150 catchments in the southern part. Possible links between debris flow and climate were investigated using two different approaches. The first approach was determining the rainfall thresholds responsible for triggering debris flow events by analysing the links between the intensity and the duration of rainfall events. The second approach used a probabilistic logit model to explore the links between the triggering of debris flow events and temperature and precipitation during the active debris flow period to identify inter-annual variability. Reanalysis data were used to document climate conditions in the two study areas.

According to the results, in 80% of all debris flow events, precipitation was recorded during the three days preceding the event. However, in most cases, the quantity of precipitation associated with triggering of the debris flow was very low. Total precipitation exceeded 10 mm in only 30% of all cases. We attribute this to the convective nature of summer precipitation, which is quite difficult to model. Probabilistic analysis of the debris flow inventory in the two regions revealed that different parameters were responsible for changes in annual debris-flow activity. In the northern part of the French Alps, the number of rainy days and the maximum daily temperature affected debris flow, while in the southern part the only significant factor was mean daily temperature during the period of debris flow activity (May–October). Model scores had an accuracy of 75% and 70% in the northern and southern Alps, respectively. Our observations revealed that the increase in the above parameters has influenced changes in debris flow activity in both regions, where the number of debris flow events has doubled over the last 35 years.

1. Introduction

Debris flows (DFs) are defined as rapid flows of saturated non-plastic debris within a steep channel (Hungr, 2005). In mountainous areas like the Alps, such events are a major threat as they periodically damage infrastructure, disrupt transportation networks (Jomelli et al., 2011) and may even cause loss of life. DFs vary significantly in frequency, magnitude, intensity, and severity. In the western part of the Alps, intense and/or long-lasting precipitation is mainly responsible for triggering DFs (Guzzetti et al., 2007). However DFs are caused by interactions between meteorological and geomorphological factors, such as the local topography or the accumulation of rock debris, which makes it difficult to understand their activity. Whatever the case, the triggering process is definitely sensitive to climate change and this fact has been confirmed by numerous palaeo-DF records reconstructed from chronostratigraphy (*e.g.*, Brazier et al., 1988; Jonasson, 1993; Blikra and Nemec, 1998; Blair, 1999; Matthews et al., 2009), lichenometry (Innes, 1985; Winchester and Harrison, 1994; Helsen et al., 2002; Jomelli et al., 2002; Jomelli, 2013), and tree ring techniques (Stoffel et al., 2005, 2008; Bollschweiler and Stoffel, 2010; Lopez Saez et al., 2011). Moreover, expected future climate change may alter the dynamics of slope processes including DFs (Jomelli et al., 2009; Chiarle et al., 2011), and therefore the frequency or magnitude of extreme DF events (Stoffel, 2010). Consequently, evaluating the link between climate and DF activity is the first step in any attempt to predict future events.

Many authors who identified links between DF and climate focused on the meteorological conditions responsible for events triggered in a single catchment or in several neighbouring catchments with similar biophysical characteristics (Pelfini and Santilli, 2008; Bocchiola et al., 2010). However, links established at local scale may not be applicable to other places where the biophysical characteristics such as elevation,

* Corresponding author. Tel.: +33 145075583.
E-mail address: pavlova@cnrs-bellevue.fr (I. Pavlova).

http://dx.doi.org/10.1016/j.geomorph.2014.04.025
0169-555X/

lithology, and vegetation are not the same. Fewer authors focused on the triggering of DFs related to climate conditions in very different catchments and at a large spatial scale. For example, regional thresholds of intensity/duration of precipitation events responsible for DFs and landslides were established by Caine (1980) and improved by Guzzetti et al. (2008). Based on this approach, the U.S. Geological Survey developed a landslide warning system with regional thresholds that take into account mean annual precipitation normalized by the number of rainy days (Wilson, 1997a). Other regional studies showed that temperature can be an important factor. Working in different glacial valleys in the Caucasus, Seynova et al. (2007) reported an increase in DF activity at a regional scale in recent decades caused by glacial retreat linked to warmer temperatures.

In the Alps, studies of a large number of catchments over a long time period are still rare (Guzzetti et al., 2007). Some authors focused on the meteorological/climatological conditions responsible for triggering DFs at a large spatial scale but only in special years such as 1987, which was characterised by a very large number of triggered events in the Swiss Alps (Haeberli et al., 1990; Zimmermann, 1990). Other authors focused on a few specific catchments (Borga et al., 2002; Fiorillo and Wilson, 2004; Stoffel and Beniston, 2006). In the French Alps, Jomelli et al. (2003, 2004, 2007, 2011) analysed links between climate conditions and different types of debris avalanches, corresponding to a shallow flow of partially- or fully-saturated debris that is not confined to an established channel (Hungr, 2005), as a function of their lithology or the nature of the accumulated debris. In most cases, extreme precipitation in summer and the number of freezing days in spring played a significant role in triggering debris avalanches. However, for confined DF events, such analyses are still lacking.

The French Alps comprise two distinct geographic areas: a humid northern part with steep narrow valleys, and a drier southern part with vast, less steeply sloped mountainsides. As it is generally assumed that significant changes in DF activity are due to different climate conditions, one can assume that the two contrasted climate conditions over the French Alps are responsible for significant variations in DF activity.

The aim of this study was to analyse the effects of the two contrasting climate conditions on DF activity. The rest of the paper is organised as follows: in Section 2, we describe the study area and the DF and meteorological data we used. In Section 3, we describe the two independent statistical methods which have been used to analyse the links among the triggering of DFs, changes in DF activity and climate conditions in the two parts of the French Alps since 1970. In Section 4, we present the links we found between DF activity and climate based on the two statistical models. In Section 5, we discuss possible causes of changes in DF activity in the last 35 years, while Section 6 concludes this paper.

2. General setting and data

2.1. Study area

The study area covers a large part of the French Alps (Fig. 1a) spanning more than 16,000 km^2, with more than 800,000 inhabitants. From an administrative point of view, the study area corresponds to three administrative districts: Savoie, Hautes-Alpes and Alpes-de-Haute-Provence (Fig. 1b). Based on climatic, economic and geographical criteria (Meyzenq, 1984; ONERC, 2008; Météo-France, 2011), the region can be divided into two sub-regions, the northern and southern French Alps (Fig. 1c), with Savoie in the north and Hautes-Alpes and Alpes-de-Haute-Provence in the south.

The northern French Alps contain two large river valleys both oriented SE–NW: the upper Isère and the Arc. The catchments of these main valleys and their tributaries cover more than 6000 km^2. The climate is closely linked with the configuration of valleys and massifs. As the main valleys in the northern region are primarily oriented westward,

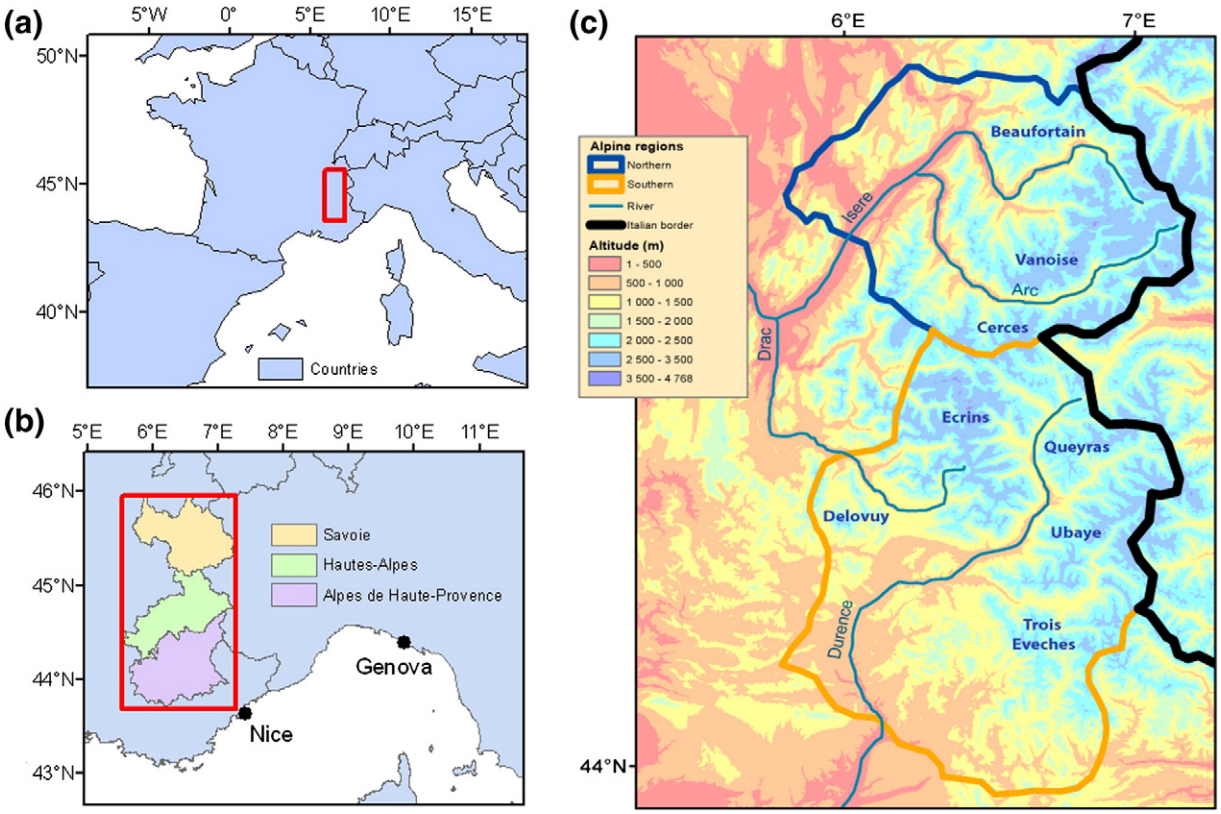

Fig. 1. Physiographic setting of the study area. (a) Location in France. (b) Administrative districts. (c) Topography.

they are exposed to the influence of the Atlantic Ocean and receive a large amount of precipitation (Météo-France, 2011). The mean annual precipitation at an elevation of 1000 m a.s.l. is about 1000 mm year^{-1} and is relatively regularly distributed throughout the year. Mean maximum temperatures are around 10 °C (Météo-France, 2011). The tree line is located between 2300 and 2400 m a.s.l. The surrounding mountain massifs are individual geographical units. The Beaufortain massif is situated north of the Isère River. It is a crystalline massif with a sedimentary cover in the south and east. Its mean elevation is 1500 m a.s.l. and its main peaks do not exceed 3000 m a.s.l. Between the two valleys is the Massif de la Vanoise, which has a mean elevation of 2000 m a.s.l. Geologically, the southeast part of this region, including the upper part of the Arc valley, consists primarily of schist. The central Massif de la Vanoise is a crystalline outbreak and the lowest northwest part is covered by sedimentary rocks. The east–west oriented Massif des Cerces is the natural border of Savoie and Hautes-Alpes, with mean elevations >2100 m. Its geological structures include a crystalline solid part (Tabor massif) and limestone, marble, and dolomite in cavity fillings such as the Massif des Cerces, le Col du Galibier, and le Mont Chaberton.

The southern French Alps are mainly under the influence of the warmer and dryer Mediterranean climate. Maximum precipitation occurs in summer (Frei and Schar, 1998) and the average annual precipitation at 1000 m a.s.l. is 700 mm. The mean maximum temperature at the same elevation is 14 °C (ONERC, 2008). Massif des Écrins is situated in the heart of the French Alps and is surrounded by the Cerces, Queyras and Ubaye mountain ridges. This massif is composed of a crystalline basement with some areas of sedimentary material, crushed or transported to the periphery of the massif. In the southeast, two distinct geographical units can be distinguished: the Queyras and the Ubaye. The former consists mostly of schist; its mean elevation is 2100 m a.s.l. The latter is composed mostly of sedimentary rocks, in particular flysch, and its mean elevation is 2400 m a.s.l. Further south, the Durance River cuts through several Alpine massifs. Further southwest, the Durance River defines a pre-alpine zone where the Massif des Trois-Évêchés and the Massif du Dévoluy are located. The former is situated on the left bank of the Durance River, is mostly comprised of marl and sandstone, and its mean elevation is 1600 m a.s.l. The latter is located on the right bank of the Durance River, and composed of limestone with a mean elevation of 1300 m a.s.l.

2.2. Historical debris flow database

DFs in the French Alps have been well documented for decades and even events that occurred centuries ago are occasionally documented. The DF data used in this study came from a survey of natural hazards conducted by the "Restoration of Mountain Land" (*Restauration des Terrains de Montagne*; RTM). This institution was set up by foresters in the 1860s and covers the entire study area. Data on natural hazards were carefully collected from scientific and technical journals, monographs by local publishers, technical reports, unpublished documents in the archives of local authorities and state agencies, and stored at RTM (Besson, 1985). Descriptors included the exact location of each catchment, and the date as well as the type of the event.

The original RTM data from the three French districts referred to more than 6000 natural disasters of different kinds. Sampling of only DF events involved several stages. We only selected events referenced as "lave torrentielles" (DF phenomena) which were distinguished from "coulee de boue" (mud flows) or "coulee de charriage" (sediment-laden floods). In addition, we made field visits to all the DF catchments selected for the present study to be sure that they were correctly classified by checking for obvious traces of DF deposits. It is important to note that in this study we do not distinguish between the different surge waves that occurred during a single DF event, as such details are not recorded in the database. In other words, the recorded frequency for each DF event should be considered as being the minimum. In addition, despite conscientious work by local monitors who recorded the DF events, it is technically impossible to account for all the DFs in the district. For this reason, the number of DF events should also be considered as being the minimum.

To avoid mistakes associated with the incorrect interpretation of DF processes recorded in the RTM database, further analyses were limited to the main period of DF activity. This is the same as the season of DF activity and is expected to be stable under stationary climate conditions (Belaya, 2005). To detect the main periods of DF activity, we examined the annual distribution of the number of DFs from the 1970s onwards. This revealed that more than 70% of all DF events occurred during the summer season. Minor activity was also observed at the end of spring (May) and at the beginning of autumn (September–October). This seasonal distribution is typical for an alpine temperate climate (Belaya, 2005). Thus, for further comparisons and analyses, only DFs triggered between May and October were taken into account.

At the end of the selection process, a DF database covering the three districts (Savoie, Hautes Alpes, and Alpes de Haute-Provence) was established. Descriptors of each DF event included the exact location of each DF catchment which made it possible to build a DF GIS database. Then the DF database was reorganised according to the location of the DF events in the two regions. Since the spring of 1970, 565 daily DF events in the two regions (282 in the north and 283 in the south) in 237 catchments (87 in the north and 150 in the south) that occurred between May and October each year were recorded.

Digitizing the DF catchment made further analyses possible, including ArcGIS calculations of specific morphometric characteristics of an individual triggering zone such as catchment area, elevations, and dominant exposure, as well as the processing of regional statistical and spatial data. These analyses were based on the Shutte Radar Topography Mission (SRTM) digital elevation model with 90 m resolution.

The lithological description was based on a simplified geological map of France (1:1,000,000, Bureau of Geological and Mining Research — BRGM). This map only shows the dominant rock distribution of the base course. To determine the potential presence/absence of permafrost, we used open access data from the European PermaNET project (Permafrost Monitoring Network) — the first continuous map of permafrost for the entire Alps (Zischg et al., 2011). The map shows the estimated likelihood of permafrost occurrence. This information was used to characterise each DF catchment in terms of the absence/presence of permafrost in the DF triggering zone.

We also used an original dataset dating from 2006 which combines vegetation classes extracted from the CORINE Land Cover, a biosphere inventory of land use maps for several European countries based on visual interpretation of satellite images at a scale of 20 m. This dataset helped us distinguish different types of land cover. For this study, CORINE Land Cover data were simplified into four classes: agricultural land, forest, grass, and absence of vegetation.

2.3. Meteorological data

Meteorological data measured within each DF catchment were often not available. For this reason, estimations were made using data in the SAFRAN system (*Systeme d'Analyse Fournissant des Renseignements Atmospheriques à la Neige*), developed and maintained by Météo-France and routinely used in operational numerical weather prediction. The SAFRAN system is a mesoscale atmospheric analysis system for surface variables. One of SAFRAN's main features is that it is based on climatically homogeneous zones and is able to take vertical variations into account. The SAFRAN estimates one value of each meteorological parameter for each climatic zone at several altitude levels. Within the climatic zone, analysed parameters depend only on elevation and aspect (Quintana-Segui et al., 2008).

The SAFRAN system (Durand et al., 1993) is a meteorological application that performs spatial analysis of weather data available from different sources such as automatic networks, the French snow weather network, and atmospheric upper-level sounding. It combines observed

information with preliminary estimations using optimal interpolation techniques (Durand et al., 1999; Vidal et al., 2010). The SAFRAN system computes vertical profiles at 6-hourly intervals with a set of meteorological variables which are ultimately projected on the corresponding mountain relief.

The SAFRAN output data are presented not in a gridded form but by climatologically homogeneous regions in which local orography is taken into account (Durand et al., 2009). The French Alps are grouped in 21 regions each about 500–1000 km^2 (Fig. 2a). Every region is split into expositions (N, E, SE, S, SW, W or flat) and elevations in 300-m slices (600–3600 m a.s.l.), as shown in Fig. 2b. In this way, the SAFRAN provides a set of distinct daily meteorological data for each exposition–elevation pair in every Alpine region.

As all the DF catchment positions were georeferenced, we were able to estimate meteorological variables for each DF catchment. Each catchment was attributed to a certain SAFRAN climate region and transformed into a set of corresponding elevation–exposition pairs based on a 90 m resolution SRTM raster. Using R-software, the required meteorological variables were computed for every elevation–exposition pair and then grouped back into a mean single variable value for each DF catchment. In order to estimate regional climate parameters, cumulated precipitation, mean precipitation, the number of rainy days, the number of rainy days with daily cumulated rainfall greater than 10/15/20/25/30/40 mm day^{-1}, and minimum and maximum temperatures for the main period of DF activity (May to October) of each year were calculated on the basis of the mean values of every DF catchment in the northern and southern regions.

The main advantage of the SAFRAN reanalysed data is clearly its continuous spatial pattern. At the same time, the main drawback is the inevitable smoothing of the data due to interpolation (Piazza et al., 2011). The SAFRAN system possesses systematic discrepancies expected either at daily or annual scales (Vidal et al., 2010).

We used the original Météo-France data for the meteorological stations Beaufort (1030 m a.s.l.) in the northern region and Embrun (871 m a.s.l.) in the southern region (Fig. 2a) in order to test the relevance of the SAFRAN data. Those meteorological stations were selected because of the availability of an uninterrupted series of daily precipitation and temperature data beginning in the 1970s and their locations close to DF catchments.

3. Methods

3.1. SAFRAN data: cross validation and regional climate trend evaluation

Before any further investigation, we checked the relevance of the SAFRAN data by comparing it with observations. An elevation–exposition pair based on the position of each meteorological station (Beaufort and Embrun) was identified and corresponding meteorological values based on the SAFRAN data were assigned. Calculated annual values were then compared with observed data for the meteorological stations concerned.

To detect possible changes in climate conditions in the northern and southern regions, different regional parameters were calculated at an annual time scale using the SAFRAN data. The next step was identifying possible climate trends since the 1970s. First we tested the values of the regional climate variables based on the SAFRAN data for normality of distribution. Then we split the variables into two periods of equal length, 1970–1987 and 1988–2005, and analysed their differences using the *t*-test (0.05 level of significance) to identify temporal increases, decreases, and non-significant changes in each region.

3.2. Statistical models to compare climate and debris flow activity

To better understand the links between the climate variables and DF activity, we 1) analysed the intensity/duration thresholds for each triggered DF event at a 6 h scale for the SAFRAN data and at a daily time scale for observed data, and 2) calculated the probability of an annual regional DF occurrence based on logistic regression analyses. This enabled us to document DF triggering conditions at a local scale and to understand why some years had more DF events than others.

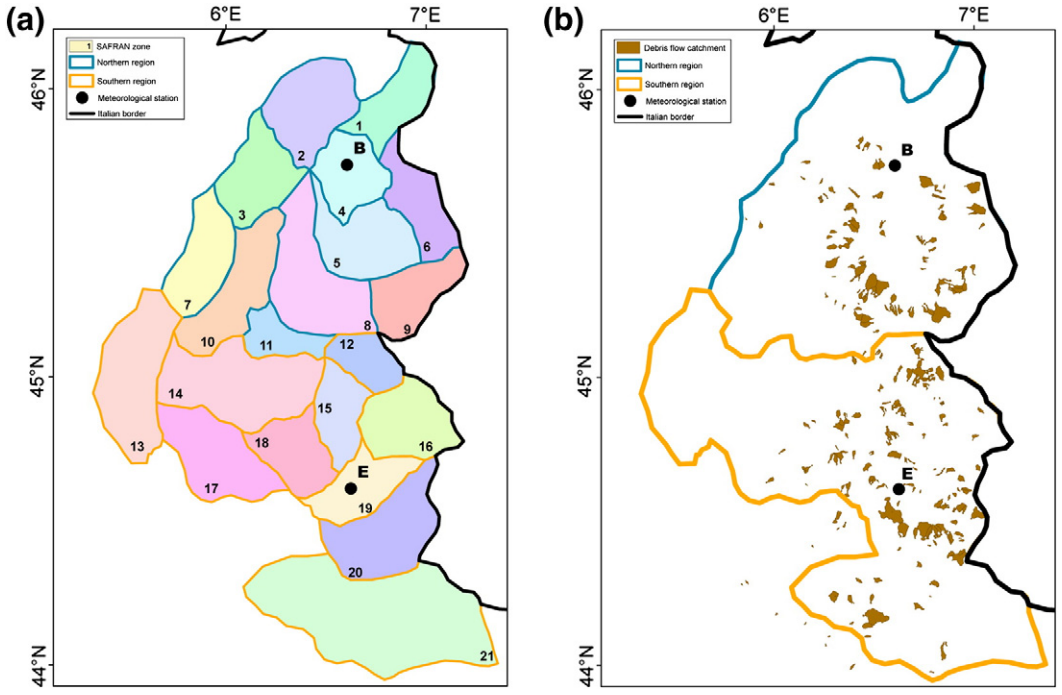

Fig. 2. Characteristics of the study area. (a) SAFRAN climatic zones and the SAFRAN data organisation scheme. (b) DF catchments. Black numbers in (a) represent the climatic zone codes — 1: Chablais; 2: Aravis; 3: Bauges; 4: Beaufortain; 5: Vanoise; 6: Haute-Tarentaise; 7: Chartreuse; 8: Maurienne; 9: Haute-Maurienne; 10: Belledone; 11: Grandes-Rousses; 12: Thabor; 13: Vercors; 14: Oisans; 15: Pelvoux; 16: Queyras; 17: Devoluy; 18: Champsaur; 19: Parpaillon; 20: Ubaye; and 21: Haut Var. Red numbers in (b) represent the most active DF catchments — 1: Torrent du Poucet; 2: Torrent de la Ravoire; 3: Torrent du Rieubel; 4: Torrent de l'Envers; and 5: Ruisseau de Cleret. B: Beaufort meteorological station. E: Embrun meteorological station.

3.2.1. Intensity/duration thresholds for extreme precipitation events

A classical approach to identify thresholds of DF occurrence consists in calculating the intensity *versus* duration (*I*/*D*) of precipitation preceding the triggering of a DF event. This method has been widely applied with some improvement (Caine, 1980; Wieczorek, 1987; Wilson, 1997b; Crosta and Frattini, 2001; Bacchini and Zannoni, 2003; Chien-Yuan et al., 2005; Guzzetti et al., 2008).

I/*D* values for DF events were obtained from observed meteorological data at the Beaufort and Embrun stations. First, we selected only DF catchments located less than 20 km from each station, and calculated the precipitation sum and the duration of total precipitation during the 72 h preceding each DF event. The 72-h period was selected after several preliminary tests from one to seven days. The distance of 20 km was determined to be the most effective radius to represent the local climate for each station after a series of preliminary tests with different distances. Second, the mean rainfall intensity per day was computed for each DF event.

The *I*/*D* threshold construction based on the SAFRAN data set was performed in a different way as the SAFRAN system makes it possible to calculate precipitation amounts in more detail. We calculated the precipitation sum and the duration of total rainfall in the 72 h preceding the DF event for every catchment in the two regions. Then a power curve describing each regional *I*/*D* threshold was fitted. This type of trend is most frequently used to describe relationships between precipitation *I*/*D* values during DF events (Guzzetti et al., 2007).

3.2.2. Logistic regression analysis

Logistic regression is frequently used to estimate the probability of an event occurrence, depending on the explanatory variables. This method has already been successfully used to estimate the climate variables responsible for triggering debris avalanches in the French Alps (Jomelli et al., 2003, 2004, 2007, 2009; Pavlova et al., 2011).

The model based on cumulative probabilities is:

$$\log it(p_i) = f(\Pr(Y_i \le i|x)) = \ln\left(\frac{p}{1-p}\right) = \alpha_i + \beta' x + e \quad (1)$$

where $f(x)$ is the logistic distribution function, Y_i is the ordered dependent variable with i varying from 1 to k, the intercept α_i varies from α_1 to α_{k-1}, β' is the slope coefficient, and e is the error (Hosmer and Lemeshow, 2000).

The logistic probability model was applied independently to each of the northern and southern regions for the warm period (May–October) of 1970–2005 to find the best climate variables to explain changes in the number of DF events per year. As each model provides only binary responses (presence/absence), a threshold of the annual number of DFs had to be set. In the north, years with fewer than seven events were coded 0, and years with more than seven events were coded 1. In the south, we used a threshold of five events so as to keep an adequate proportion of years with and without events in each region. Without this distinction, the model would overestimate one of the groups (either presence or absence) and would be unable to correctly predict the annual probability of DFs.

Different climate variables tested included the precipitation sum, the number of rainy days as well as the number of rainy days with daily cumulative rainfall greater than 10/15/20/25/30/40 mm day^{-1} for each year. The regional temperature parameters included mean daily minimum/mean/maximum values and positive degree days for each year.

To check the quality of the model, several standard tests were conducted for each logistic regression and the relative weights of each climate variable were then compared to select the most significant model. A variable was considered significant if chi-squared values differed from 0 and the corresponding *p*-value was less than 0.05. The higher the absolute value of the parameter coefficient, the higher the weight of the corresponding variable.

The percentage of correctly classified observations for the different explanatory climatic parameters was computed and also used to choose the best model. If the final percentage score was higher than 50%, the model was considered to be significant.

4. Results

4.1. Spatial and temporal variability of debris flow occurrence

DF catchments exhibited a strong geomorphological variability in the two regions of the French Alps (Fig. 3). More than 90% of the DF catchment areas for both regions do not exceed an area of 10 km^2 (Fig. 3a). The dominant aspect orientation of the catchment (Fig. 3c) in the northern region is north and west (16% and 26%, respectively), while in the southern region the dominant aspect orientations are south and southwest (25% and 26%, respectively). A pie-chart (Fig. 3b) of altitudinal distribution clearly shows that in the southern region, DFs are triggered in higher catchments than in the northern region. The minimum elevation corresponding to the highest point of a deposit zone was below 1000 m in 55% of the cases in the northern region, while in the southern region, the majority (86%) is above 1000 m.

In the northern region, more than half of the DF catchments (56%) do not go above the tree line limit, and remain in the forest zone. Conversely, in the southern region, most DF catchments occupy grasslands (23%) and vegetation-free zones (49%) above the tree line (Fig. 3d). Schist material covers nearly half the territory of the northern region, including the Massifs de la Vanoise and Cerces and is dominant in 41% of all DF catchments (Fig. 3e). The limestone formation provides solid material for 34% of the catchments. A vast part of the southern region is composed of limestone, which is a dominant lithological type in 47% of all catchments in this zone. Schist from the Massifs of Cerces and Queyras supplies 23% of the DFs in this zone. Another 20% of the catchments consist primarily of sandstone from the Massifs des Ecrins, Trois Eveches and Delovuy.

Descriptive analyses confirmed that the northern and southern regions differ considerably in the individual characteristics of their catchments. A typical DF catchment in the northern region is located on schist, in a forested zone, with westerly exposure, with a depositional zone below 1000 m a.s.l. In the southern region, the majority of DF catchments are situated in vegetation-free areas on limestone with dominant southerly exposure above 1000 m a.s.l.

The next step was a regional investigation of DF activity over time. Although the northern and southern French Alps are neighbouring regions, regional DF activity varied significantly over time (Fig. 4). Although the numbers of events in the two regions were nearly the same (57% of all events occurred in the north) there are many more catchments in the south, so each individual southern catchment is less active. However, major peaks in the number of events in the two regions were nearly the same, *i.e.*, in 1987, 1995 and 2005. When the database was split into two periods (1970–1987 and 1988–2005), a significant increase in DF events was observed after the mid-1980s. This trend was confirmed by *t*-tests (0.05 level of significance), which revealed significant differences between the mean annual DF numbers before and after 1987.

The best observed and documented activity occurred in the largest and the most dangerous catchments: Torrent du Poucet, 28 events; Torrent de la Ravoire, 25 events; Torrent du Rieubel, 17 events; and Torrent de l'Envers and Ruisseau de Cleret, 15 events (Fig. 2a). In the remaining catchments, only one or two DF events have been recorded during the last 35 years. In the north, the mean regional number of DF events in each catchment was 2.9 (standard deviation ~ 4); in the south, the mean regional number of DF events was 1.6 (standard deviation ~ 1). Consequently, it was difficult to distinguish the frequency of DF events in individual catchments for a particular period.

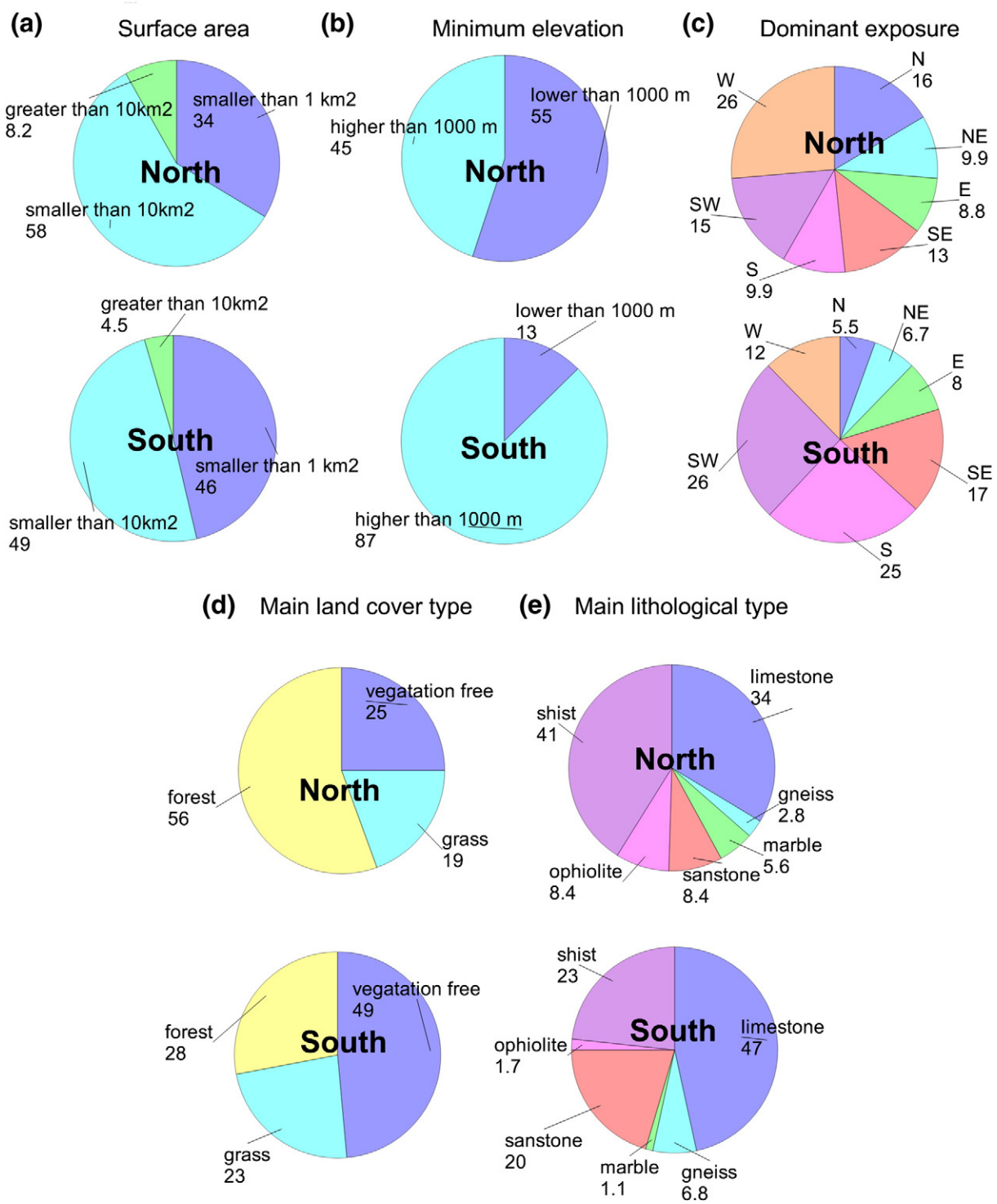

Fig. 3. Mean catchment characteristics of the northern and southern debris flow regions. (a) Surface area. (b) Minimum elevation. (c) Dominant exposure. (d) Main land cover type. (e) Main lithological type. The numbers under each pie-chart class show the percentage of each feature in the region.

4.2. SAFRAN data: cross validation and evaluation of regional climate trends

Fig. 5 shows a 10-year extract (1971–1980) of a comparison between a series for the Beaufort and Embrun meteorological stations together with the corresponding SAFRAN data. Except for a few small details, there was a substantial overlap between the SAFRAN and observed data at an annual scale. SAFRAN precipitation sums were slightly higher for Beaufort and Embrun, but less than 5%. Observed maximum temperatures were accurately represented by the SAFRAN data, and differences were less than 2%. The trend of slightly lower temperature and higher precipitation in the SAFRAN data was observed at all meteorological stations. According to Quintana-Segui et al. (2008), the differences in temperature and precipitation are largely due to the interpolation techniques used for the SAFRAN data.

Fig. 6 shows annual variation in the main climate characteristics. The mean air temperature during the warm period in the two regions were quite close: the maximum temperature was approximately

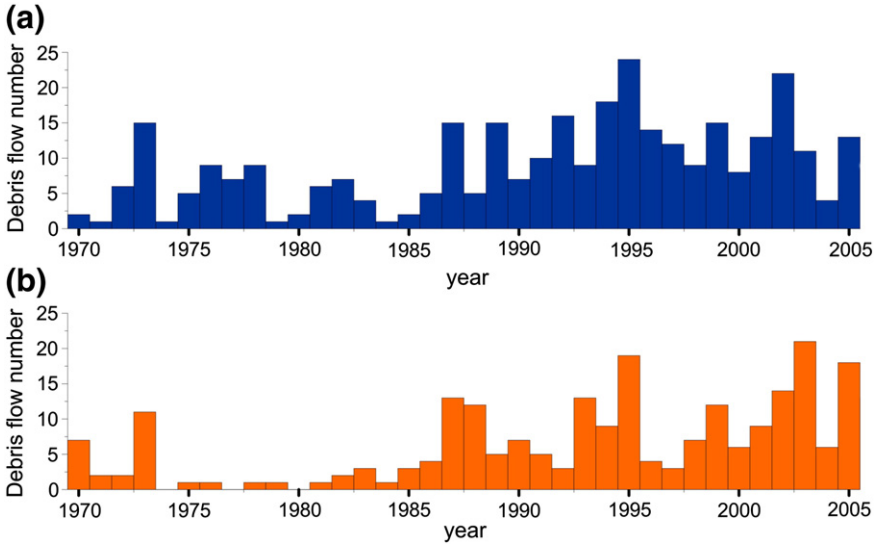

Fig. 4. Debris flow distribution since the 1970s in the northern (a) and southern (b) regions of the French Alps.

11 °C (11.2 °C in the north and 10.8 °C in the south) and the minimum temperature was approximately 4.5 °C (4.7 °C in the north and 4.6 °C in the south).

Table 1, which is based on the SAFRAN results, shows that, since the mid-1980s, there has been a significant increase in temperatures during May to October in the two regions (Student's *t*-test; 0.05 level of significance). This trend agrees with other studies covering the entire European Alps using homogenised instrumental time series (Beniston et al., 1997; Bohm et al., 2001; Beniston et al., 2011).

According to the SAFRAN data, the changes in precipitation were more complex. A higher sum of precipitation was observed in the northern region, with an average of 670 mm year^{-1}, *versus* 580 mm year^{-1} in the southern region (Fig. 6). There were slightly more rainy days in the northern region (88 rainy days) than in the southern region (79 rainy days). During the period 1970–2005, there were 21 days per year on average with a total daily precipitation >10 mm in the northern region and 17 such days in the southern region. On average, there were nine days per year with a total daily precipitation >20 mm in the north, and seven in the south. For the last 35 years, the mean sum of precipitation has remained stationary from May to October in both regions (Table 1). There was a significant increase in the number of rainy days, but no significant changes in daily precipitation above the thresholds in terms of the number of days with precipitation >10/20 mm day^{-1} for each year.

4.3. Statistical models to compare climate parameters and debris flow activity

4.3.1. Debris flow triggering condition estimated from rainfall intensity/duration thresholds

We first estimated *I*/*D* thresholds on the basis of observed meteorological daily data. DF catchments located within a radius of 20 km from each meteorological station were selected (eight DF catchments for the Beaufort station in the northern region and 26 for Embrun in the southern region). The mean hourly *I*/*D* of each DF event was calculated for the period 1970–2005. More than 80% of all the DF events recorded at the two stations were characterised by an intensity of less than 1 mm h^{-1} and the maximum intensity did not exceed 2 mm h^{-1}. Most rainfall events did not last more than two days.

Unlike with observed meteorological data, using the SAFRAN system we were able to calculate *I*/*D* values for each DF event in all 237 catchments. We plotted all the DF events which occurred during the main

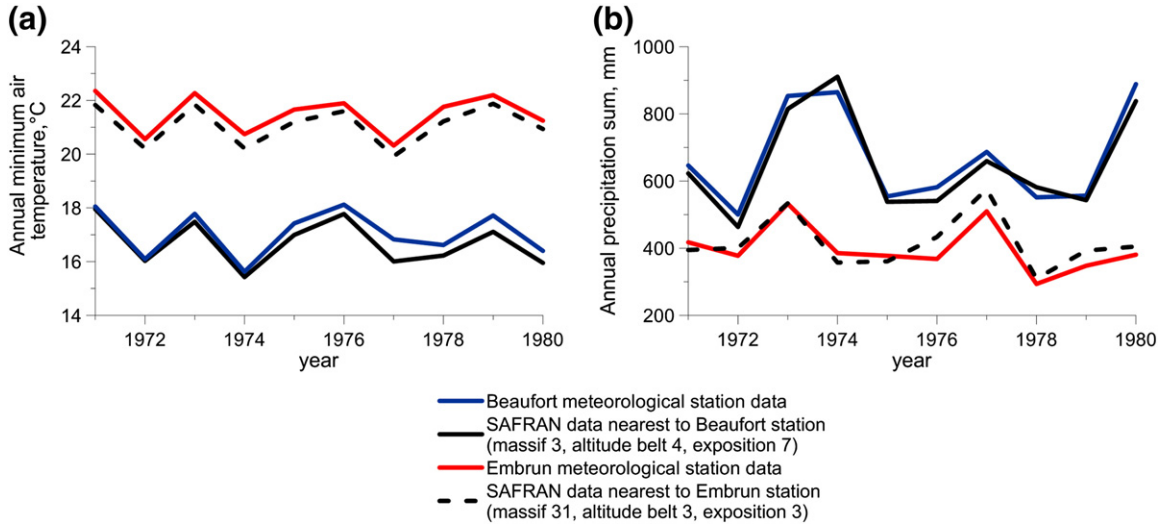

Fig. 5. Comparison of data from the Beaufort and Embrun meteorological stations and the corresponding SAFRAN values for May to October of each year, for the period 1971–1980. Parameters are maximum air temperature (a) and precipitation sum (b).

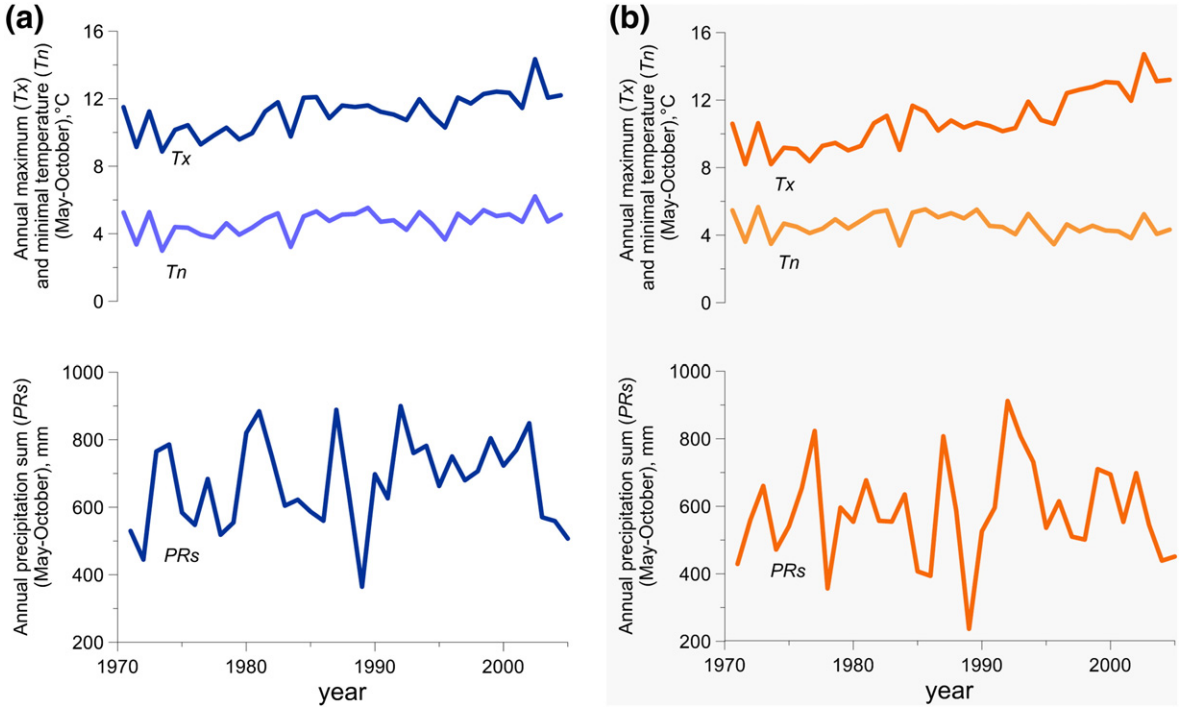

Fig. 6. Distribution of temperature and precipitation parameters in the northern (a) and southern (b) regions of the French Alps for the period 1970–2005 based on the SAFRAN data. *Tx* — mean maximum daily temperature; *Tn* — mean minimum daily temperature; *PRs* — precipitation sum. All parameters were calculated for the period May to October of each year.

period of activity since 1970 as a function of the precipitation characteristics of the SAFRAN data corresponding to DF catchments (Fig. 7). The main trend was a decrease in intensity but an increase in duration. According to the SAFRAN data, 80% of DF events were triggered by precipitation during the 72 h preceding the event. However, a total precipitation sum of 1–10 mm per rainstorm was recorded for nearly half the events. Only 30% of all events were triggered by rainstorms with a total precipitation of more than 10 mm, and 10% with >30 mm per rainstorm.

Most DF events in the two Alpine regions were thus associated with low-intensity (<4 mm h^{-1}) and relatively short precipitation (less than one day). Five percent of the rainfall events lasted more than 24 h but less than 48 h. In the southern region, the percentage of DF events associated with intense precipitation *i.e.* >4 mm h^{-1} was low (10%), but higher than in the northern region (3%). However, the difference in the distribution of the DF events between two regions was not significant. Tests comparing the *I*/*D* of DF events revealed no differences between catchments with different types of dominant lithology.

To quantify the regional *I*/*D* threshold, we applied a power low equation for DF events caused by extreme precipitation. As the minimum extreme rainfall threshold for the French Alps corresponds to

Table 1
Results of significance tests (0.05 level of significance) of the climate parameters for the periods 1970–1987 and 1987–2005 based on the mean from the annual SAFRAN data. *PRs* — precipitation sum; *Nrd* — number of rainy days; *Nrd 10/20* — number of days with precipitation >10/20 mm day^{-1}; *Tn* — mean minimum daily temperature; *Tx* — mean maximum daily temperature. All parameters were calculated for the period of May to October in each year.

Climate parameter	P-value	Difference	Mean 1970–1987	Mean 1987–2005	Significance trend
Northern region					
PRs	0.492	−31.2	654.6	685.8	No change
Nrd	0.001	−9.1	84.2	93.3	Increase
Nrd > 10	0.621	−0.8	21.1	21.9	No change
Nrd > 20	0.87	−0.17	8.5	8.6	No change
Tn	0.016	−0.6	4.4	5.0	Increase
Tx	0.001	−1.3	10.5	11.8	Increase
Tm	0.001	−0.9	7.4	8.3	Increase
Southern region					
PRs	0.649	−22.4	569.2	591.6	Equal
Nrd	0.001	−12.0	73.2	85.2	Increase
Nrd > 10	0.873	−0.2	17.5	17.7	Equal
Nrd > 20	0.586	0.6	7.7	7.1	Equal
Tn	0.365	0.2	4.7	4.5	Equal
Tx	<0.0001	−2.1	9.7	11.8	Increase
Tm	0.003	−0.8	7.2	8.0	Increase

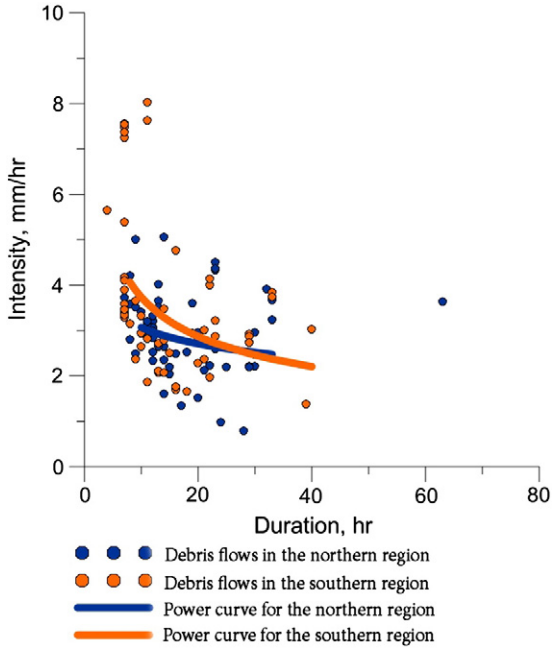

Fig. 7. Intensity (*I*) and duration (*D*) of precipitation (only rainstorms with precipitation sums greater than 10 mm) preceding each debris flow event in the northern and southern regions based on the SAFRAN data.

10 mm (Jomelli et al., 2007), all DFs with total precipitation sums greater than 10 mm were taken into account, making a total of 193 DF events for the two regions.

Fig. 7 shows the following two power curves:

$$I = 4.64D^{-0.18} \text{ for the northern French Alps} \quad (2)$$

$$I = 8.96D^{-0.38} \text{ for the southern French Alps.} \quad (3)$$

There is a difference in the coefficient and exponent of the equations for the northern and southern regions. This difference is visible during the first 24 h after DF triggering and smooths out with a longstanding rainfall duration (Fig. 7). As *I*/*D* thresholds presented in Eqs. (2) and (3) do not correspond exactly to the methodology recently used by other authors (*e.g.* Guzzetti et al., 2007), these values cannot be directly compared with regional thresholds for other Alpine regions.

4.3.2. Inter-annual variability of debris flows from logistic regression analysis

Results of the inter-annual regional tests are presented in Table 2. In the southern region, the best results (*i.e.* the highest percent of correctly predicted DFs with a significant *p*-value per year), were obtained with the mean annual temperature (*Tm*).

The linear equation of the logistic probability model from Eq. (1) for the southern region is:

$$\text{Annual debris flow probability}\left(>5 \text{ events year}^{-1}\right) = 1/\{1 + \exp[-(-13.46 + 1.76Tm)]\}. \quad (4)$$

Results for the northern region were somewhat more complex: in addition to the same significant temperature parameters as in the south, there was one significant precipitation parameter — the number of rainy days per year (*Nrd*). This bivariate model with two explanatory factors gave a higher percent of correctly predicted DFs than tests where these climate parameters were examined separately.

The best linear equation of the logistic probability model from Eq. (1) for the northern region is:

$$\text{Annual debris flow probability}\left(>7 \text{ events year}^{-1}\right) = 1/\{1 + \exp[-(-21.91 + 0.14Nrd + 0.9Tx)]\}. \quad (5)$$

Model parameters were significant at the 0.05 level and revealed a high chi-square score (Table 2). More than 65% of the model predictions for years with low activity were correct in the two regions: less than seven events in the northern Alps and five events in the southern Alps. The predictions for years with high activity (more than seven events in the northern Alps and five events in the southern Alps) were 75% and 70% correct, respectively.

Fig. 8 shows the annual probability of DF activity as a function of *Nrd* and *Tx* for the northern region, and as a function of *Tm* for the southern region. The probability of DF increased considerably with an increase in both parameters. In the northern region, the probability of DF events >0.7 was positive when *Nrd* was >85 and *Tx* was >12 °C. The highest probability values in the south were for years in which *Tm* was >8.5 °C.

5. Discussion

5.1. Climatic/geomorphic parameters responsible for DF years

It is well known that two conditions are required for DFs to be triggered (Caine, 1980; Johnson and Rodine, 1984; Van Steijn, 1996; Iverson, 1997): long-duration or high-intensity rainfall and large quantities of available rock debris. Consequently, to perfectly understand the phenomena that trigger DFs, both climatic and geomorphic parameters have to be included in the same model.

The quantification of stored rock debris is undoubtedly the most difficult problem to resolve. Some authors attempted to quantify this storage using direct observations in the channel (Jakob et al., 2005; Veyrat-Charvillon and Menier, 2006; Conway et al., 2010; Zhang and Shen, 2011); others used analyses of susceptibility zones (Borga et al., 2002; Magliulo et al., 2008; Loye et al., 2011) or estimations of DF volume (Rickenmann, 1999; Gartner et al., 2008; Chang et al., 2011; Theule et al., 2012). However, these approaches cannot reasonably be applied when a study is conducted at a large scale (Brochot et al., 2002). To compensate for this difficulty, some authors took storage

Table 2
Results of logit models for the northern and southern regions. Significant parameters are in bold. *PRs* — precipitation sum; *Mean rr* — mean positive daily precipitation; *Nrd* — number of rainy days; *Nrd > 10/20* — number of days with precipitation >10/20 mm day^{-1}; *Tn*, *Tm*, and *Tx* — mean minimal, mean, and mean maximum daily temperature. All parameters were calculated for the period May to October of each year.

Meteorological parameter	Coefficient value	Wald Chi^2	*Pr > Chi*^{2}	% correct 0	% correct 1	% correct all
Northern region						
PRs	0.201	1.102	0.294	43.75	75.00	61.11
Mean rr	0.462	3.041	0.081	56.25	75.00	66.67
Nrd	**0.651**	**5.701**	**0.017**	**56.25**	**75.00**	**66.6**
Nrd > 10	0.186	0.942	0.332	25.00	80.00	55.56
Nrd > 20	0.114	0.372	0.542	12.50	80.00	50.00
Tn	0.322	2.478	0.115	43.75	80.00	63.89
Tm	**0.428**	**3.802**	**0.051**	**50.00**	**75.00**	**63.89**
Tx	**0.513**	**4.812**	**0.028**	**50.00**	**75.00**	**63.89**
Best model						
Nrd	**0.659**	**5.652**	**0 017**	**68.75**	**75.00**	**72.22**
Tx	**0 577**	**4.389**	**0 036**			
Southern region						
PRs	0.021	0.013	0.909	88.89	11.76	51.43
Mean rr	−0.088	0.219	0.64	66.67	47.06	57.14
Nrd	0.229	1.354	0.245	66.67	47.06	57.14
Nrd > 10	0	0	0.999	100.00	0.00	51.43
Nrd > 20	0.011	0.003	0.955	100.00	0.00	51.43
Tn	0.23	1.391	0.238	66.67	47.06	57.14
Tx	**0.82**	**7.712**	**0.005**	**77.78**	**52.94**	**65.71**
Best model						
Tm	**0.835**	**7.731**	**0.005**	**66.67**	**70.59**	**68.57**

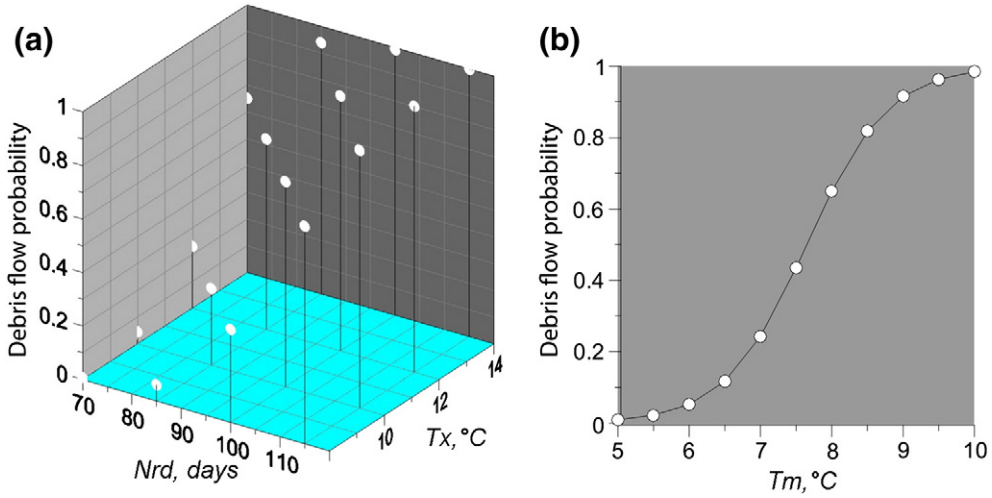

Fig. 8. Annual probability of debris flows in the northern (a) and southern (b) regions of the French Alps. *Nrd* — number of days with precipitation per year; *Tx* — mean maximum daily temperature; *Tm* — mean daily temperature.

into account indirectly by assuming that storage depends on the size of other geometric parameters, such as the extent of the part of the watershed that contributes to the creation of storage. For example, Jomelli et al. (2003) showed that the probability of triggering a DF event in the French Alps increased in relation to the size and elevation of the rock wall above the cone, suggesting a link between the storage of rock debris and the geomorphic characteristics of the catchment. Nevertheless, in most cases, such a parameter is very difficult to estimate and is associated with major uncertainties, and consequently cannot reasonably be used in a regional approach.

In the present analysis, we chose to work from a large dataset distributed over a vast spatial area and conducted two distinct analyses based on *I*/*D* of precipitation and on estimated probabilities at an annual time scale both analysed over a 35 year period. This choice enabled us to more accurately document the quantity of stored debris mobilised in each event. By dealing with a large spatial and temporal scale, we captured the entire variability of catchments with both moderate and large debris storage. Moreover, the analyses of individual catchments showed that most debris storage consists of schist and limestone. We consider that DF catchments had an unlimited supply of stored debris throughout the period investigated.

5.2. Data accuracy

In this study, we analysed DF activity in the French Alps based on the unique historical database containing more than 550 DF events during last four decades. This database originally came from the RTM, which was confirmed by the process type registered *in situ*, DF catchment spatial distribution and temporal occurrence of DF events. In addition, the SAFRAN system provides meteorological data for every DF case. These datasets allowed us to perform a regional investigation, which was rare in the literature (Tropeano and Turconi, 2004; Marchi and Cavalli, 2007).

An important question concerns the accuracy of DF survey data, as this could influence the accuracy of the model results. The RTM service was established in the late 19th century and has continually improved the quality of its data. One of the most recent quality leaps was made after a dramatic snow avalanche in February 1970, which caused the death of 39 people in Val d'Isère (Savoie, France). Since then, the French government recognised that a natural hazard database would be useful for risk management and commissioned a more accurate survey of natural hazards including DFs. This is why we did not analyse events before 1970.

Despite conscientious work by those who recorded natural hazards *in situ*, there may also be discrepancies concerning the exact date of a DF event. To compensate for this difficulty, the *I*/*D* method was based on a large dataset, in which we assumed that the impacts of inexact cases were limited. Logistic analyses were conducted at an annual time scale assuming that, at this scale, errors do not affect the results.

According to the DF database, the number of events in both regions was nearly the same although there is only half the number of catchments in the southern region. It is also well known that the southern Alps has less infrastructure than the northern Alps, so many active catchments in uninhabited areas are not recorded in the RTM database. This fact certainly influences the results, but still it is hard to measure the incertitude of such an impact.

Results based on *I*/*D* tests showed that most DFs were triggered by a small amount of precipitation and short duration rainfall events. At the same time, the relationships between DF occurrence and climate based on a logistic annual model revealed different variables in the two regions. Initially, the role these factors played in DF occurrence may seem dubious, but can be explained from the specificity of the data on the regional meteorological situation and the time scale of our model.

The analyses conducted at an annual scale using logistic regression tests in the northern region revealed the *Nrd* to be a main driver of DF variability. This variable is combined with an increase in *Tx* which provides indirect evidence for the formation of convective precipitation (Plaut and Simonnet, 2001; Garçon et al., 2010). The total precipitation in the southern region of the French Alps was less than in the north. The southern region is strongly influenced by the Mediterranean climate, which includes the strongest storm activity, *i.e.*, convective precipitation, especially in summer or on hot days or nights (Salameh, 2008; Gottardi et al., 2012). These storms are responsible for the frequent extreme precipitation that triggers DF events. The fact that we did not identify any significant parameters for extreme precipitation such as the number of days with precipitation >10/20 mm day^{-1}, is probably due to the difficulty involved in measuring convective precipitation at a daily time scale even with the SAFRAN reanalysed data. In the future, radar images should help to more accurately estimate the influence of precipitation (Berg et al., 2013).

Another question concerns the relevance of the exact location of the division between the northern and southern regions. Indeed, despite clear climate differences between the northern part and the southern part of the French Alps, they do not necessarily match the border between the Hautes-Alpes and Savoie districts. To test this hypothesis, we shifted the limit of the northern region southwards. As a result, about 30% of DF data previously considered to come from the southern

region but now located in the northern part of Hautes-Alpes district were included in the data set of the new northern part, and the models were run again. The results did not reveal any significant change either in the trend of *I*/*D* tests or in the nature of the climate parameters used in the logistic regression analyses. The district of Hautes-Alpes appears to be an intermediate zone in DF dynamics, as well as a threshold climate zone between the humid northern Alps and the Mediterranean southern Alps.

5.3. Current climate changes and debris flow activity

The climate changes that took place during the course of the 20th century were recorded in all parts of the Alpine mountainous region (Bohm et al., 2001; Beniston et al., 2011). Since the 1980s, these changes have become even more marked. Using SAFRAN reanalysis data, we investigated trends in the main meteorological parameters in the northern and southern French Alps and observed significant changes in specific climate variables in the last four decades. According to logistic models, such an increase also increases the probability of DFs. In agreement with this probabilistic modelling approach, we observed a two-fold increase in the number of DFs since the 1980s.

Considering annual uncertainties in the DF database, one may wonder if the increase in the number of DF events over the last 35 years revealed by our results is significant. Even if bias in our DF dataset cannot be excluded, we assume that this increase in DF activity since the 1980s could also be due to climate changes in the Alps, because the increase occurred in both regions, and the survey was conducted by different observers. Moreover, there are several catchments in which more than 10 events were recorded. Looking closer at individual chronologies of those well-documented catchments, we observed the same trend to an increase in DF events since the mid-1980s.

6. Conclusions

Significant climate changes observed in both the northern and southern French Alps have caused major changes in the environment, including DF activity. We examined the link between DF activity and climate parameters in the two regions of the French Alps over last the four decades (1970–2005).

A regional approach required a large DF database as well as an accurate meteorological data set. More than 550 DFs triggered since 1970 in the northern and southern French Alps were selected from an original RTM survey database. Meteorological data reanalysed by the SAFRAN system was chosen as being the most appropriate for this kind of investigation.

The aim of this research was to accurately describe changes in regional DF activity. Two methods were applied at different time scales: (a) determining the regional *I*/*D* thresholds of rainfall events that trigger a DF event at a daily time scale, and (b) calculating the probability of regional DF activity at an annual time scale.

The first classical precipitation *I*/*D* approach revealed slight differences in triggering conditions in the two regions. Calculating the probability of DF activity revealed that in the northern region, which has a greater annual precipitation sum than the southern region, DF activity increases with an increase in the number of rainy days and the maximum daily temperature during the warm season. This is indirect evidence for the formation of convective precipitation. In the southern region of the French Alps, the total precipitation sum is less than in the north. This region is strongly influenced by the Mediterranean climate, which includes the strongest storm activity, *i.e.*, convective precipitation in the summer, especially on hot days or warm nights. This could explain why, according to the best model, the southern region is more susceptible to DF activity when the mean daily temperature increases.

Acknowledgements

This research was conducted in the Laboratory of Physical Geography (LGP, CNRS-Meudon) within the framework of the following projects: ACQWA (Assessing Climate impacts on the Quantity and quality of WAter; EU FP7), ARNICA (Assessment of Risks on transportation Networks resulting from slope Instability and Climate change in the Alps; ERANET CIRCLE-MOUNTAIN (2010–2013)) and SCAMPEI (Scénarios Climatiques Adaptés aux zones de Montagne: Phénomènes extrêmes, Enneigement et Incertitudes; ANR-08-VULN-0009-01). We would like to offer special thanks to the Restauration des Terrains de Montagne in the districts of Savoie, Hautes-Alpes and Alpes-de-Haute-Provence for allowing us to use their database.

We would also like to thank the editor Takashi Oguchi and two anonymous reviewers for their very helpful comments, which gave us a possibility to address several issues that were initially overlooked.

References

Bacchini, M., Zannoni, A., 2003. Relations between rainfall and triggering of debris-flow: case study of Cancia (Dolomites, Northeastern Italy). Nat. Hazards Earth Syst. Sci. 3, 71–79.
Beniston, M., Diaz, H.F., Bradley, R.S., 1997. Climatic change at high elevation sites: an overview. Clim. Chang. 36, 233–251.
Beniston, M., Stoffel, M., Hill, M., 2011. Impacts of climatic change on water and natural hazards in the Alps: can current water governance cope with future challenges? Examples from the European "ACQWA" project. Environ. Sci. Policy 14, 734–743.
Berg, P., Moseley, C., Haerter, J.O., 2013. Strong increase in convective precipitation in response to higher temperatures. Nat. Geosci. 6, 181–185.
Belaya, N., 2005. Modeling of Debris Flow Annual Distribution in Mountainous Regions (PhD thesis. In Russian, 187 pp.).
Besson, L., 1985. Les risques naturels. Rev. Géogr. Alpine 73, 321–333.
Blair, T.C., 1999. Sedimentology of the debris-flow dominated Warm Spring Canyon alluvial fan, Death Valley, California. Sedimentology 46, 941–957.
Blikra, L.H., Nemec, W., 1998. Postglacial colluvium in western Norway: depositional processes, facies and palaeoclimatic record. Sedimentology 45, 909–959.
Bocchiola, D., Mihalcea, C., Diolaiuti, G., Mosconi, B., Smiraglia, C., Rosso, R., 2010. Flow prediction in high altitude ungauged catchments: a case study in the Italian Alps (Pantano Basin, Adamello Group). Adv. Water Resour. 33, 1224–1234.
Bohm, R., Auer, I., Brunetti, M., Maugeri, M., Nanni, T., Schoner, W., 2001. Regional temperature variability in the European Alps: 1760–1998 from homogenized instrumental time series. Int. J. Climatol. 21, 1779–1801.
Bollschweiler, M., Stoffel, M., 2010. Changes and trends in debris-flow frequency since A.D. 1850 — results from the Swiss Alps. The Holocene 20, 907–916.
Borga, M., Dalla Fontana, G., Cazorzi, F., 2002. Analysis of topographic and climatic control on rainfall-triggered shallow landsliding using a quasi-dynamic wetness index. J. Hydrol. 268, 56–71.
Brazier, V., Whittington, G.W., Ballantyne, C.K., 1988. Holocene debris cone evolution in Glen Etive, Western Grampian Highlands, Scotland. Earth Surf. Process. Landf. 13, 525–531.
Brochot, S., Marchi, L., Lang, M., 2002. Debris flow volume assessment: available methods and application to the Poucet torrent (Savoy, France). Bull. Eng. Geol. Environ. 61, 389–402.
Caine, N., 1980. The rainfall intensity–duration control of shallow landslides and debris-flows. Geogr. Ann. 62A, 23–27.
Chang, C.W., Lin, P.S., Tsai, C.L., 2011. Estimation of sediment volume of debris flow caused by extreme rainfall in Taiwan. Eng. Geol. 123, 83–90.
Chiarle, M., Geertsema, M., Mortara, G., Clague, J.J., 2011. Impacts of climate change on debris flow occurrence in the cordillera of western Canada and the European Alps. In: Genevois, R., Hamilton, D.L., Prestininzi, A. (Eds.), Proceedings 5th Inter. Conf. on Debris Flow Hazards. La Sapienza, Roma, pp. 45–52.
Chien-Yuan, C., Tien-Chien, C., Fan-Chieh, Y., Wen-Hui, Y., Chun-Chieh, T., 2005. Rainfall duration and debris-flow initiated studies for real-time monitoring. Environ. Geol. 47, 715–724.
Conway, S.J., Decaulne, A., Balme, M.R., Murray, J.B., Towner, M.C., 2010. A new approach to estimating hazard posed by debris flows in the Westfjords of Iceland. Geomorphology 114, 556–572.
Crosta, G.B., Frattini, P., 2001. Rainfall thresholds for triggering soil slips and debris flow. In: Mugnai, A., Guzzetti, F., Roth, G. (Eds.), Proceedings 2nd EGS Plinius Conference on Mediterranean Storms, pp. 463–487 (CNR-GNDCI Publication, Siena).
Durand, Y., Brun, E., Mérindol, L., Guyomarc'h, G., Lesaffre, B., Martin, E., 1993. A meteorological estimation of relevant parameters for snow models. Ann. Glaciol. 18, 65–71.
Durand, Y.G., Giraud, G., Brun, E.L., Merindol, L., Martin, E.A., 1999. A computer-based system simulating snowpack structures as a tool for regional avalanche forecasting. J. Glaciol. 45, 469–484.
Durand, Y., Giraud, G., Laternser, M., Etchevers, P., Mérindol, L., Lesaffre, B., 2009. Reanalysis of 47 years of climate in the French Alps (1958–2005): climatology and trends for snow cover. J. Appl. Meteorol. Climatol. 48, 2487–2512.
Fiorillo, F., Wilson, R.C., 2004. Rainfall induced debris flows in pyroclastic deposits, Campania (southern Italy). Eng. Geol. 75, 263–289.

Frei, C., Schar, C., 1998. A precipitation climatology of the Alps from high-resolution rain-gauge observations. Int. J. Climatol. 18, 873–900.
Garçon, R., Garavaglia, F., Gailhard, J., Paquet, E., Gottardi, F., 2010. Homogeneous samples and reliability of probabilistic models: using an atmospheric circulation patterns sampling for a better estimation of extreme rainfall probability. NICDS Workshop: Statistical Methods for Geographic and Spatial Data in the Management of Natural Resources. EDF-DTG, (Montréal, 39 pp.).
Gartner, J.E., Cannon, S.H., Santi, P.M., Dewolfe, V.G., 2008. Empirical models to predict the volumes of debris flows generated by recently burned basins in the western U.S. Geomorphology 96, 339–354.
Gottardi, F., Obled, C., Gailhard, J., Paquet, E., 2012. Statistical reanalysis of precipitation fields based on ground network data and weather patterns: application over French mountains. J. Hydrol. 432–433, 154–167.
Guzzetti, F., Peruccacci, S., Rossi, M., Stark, C.P., 2007. Rainfall thresholds for the initiation of landslides in central and southern Europe. Meteorog. Atmos. Phys. 98, 239–267.
Guzzetti, F., Peruccacci, S., Rossi, M., Stark, C.P., 2008. The rainfall intensity–duration control of shallow landslides and debris flows: an update. Landslides 5, 3–17.
Haeberli, W., Rickenmann, D., Zimmermann, M., Rossli, U., 1990. Investigation of 1987 debris flows in the Swiss Alps: general concept and geophysical soundings. IAHS Publ. 194, 303–310.
Helsen, M.M., Koop, P.J.M., Van Steijn, H., 2002. Magnitude–frequency relationship for debris flows on the fan of the Chalance torrent, Valgaudemar (French Alps). Earth Surf. Process. Landf. 27, 1299–1307.
Hosmer, D., Lemeshow, S., 2000. Applied Logistic Regression, Second ed. John Wiley & Sons Incorporated Publication, New York (373 pp.).
Hungr, O., 2005. Classification and terminology. In: Jakob, M., Hungr, O. (Eds.), Debris Flow Hazards and Related Phenomena. Springer, Berlin, pp. 10–23.
Innes, J.L., 1985. Lichenometric dating of debris-flow deposits on Alpine colluvial fans in Southern Norway. Earth Surf. Process. Landf. 10, 519–524.
Iverson, R.M., 1997. The physics of debris flows. Rev. Geophys. 35, 245–296.
Jakob, M., Bovis, M., Oden, M., 2005. The significance of channel recharge rates for estimating debris flow magnitude and frequency. Earth Surf. Process. Landf. 21, 755–766.
Johnson, A.M., Rodine, J.R., 1984. Debris flow. In: Brundsen, D., Prior, D.B. (Eds.), Slope Instability. Wiley and Sons, London, pp. 257–361.
Jomelli, V., 2013. Lichenometric dating of debris flow deposits with an example in part of the French Alps. In: Bollschweiler, M., Stoffel, M., Rudolf-Miklau, F. (Eds.), Tracking Torrential Processes on Fans and Cones. Springer, Berlin, Heidelberg, New York, pp. 211–224.
Jomelli, V., Bertran, P., Kunesch, S., 2002. Le cône de la Momie: un nouveau type de dépôt proglaciaire mis en place depuis la fin du Petit Age Glaciaire. Quaternaire 13, 257–263.
Jomelli, V., Chochillon, C., Brunstein, D., Pech, P., 2003. Hillslope debris flows occurrence since the beginning of the 20th century in the French Alps. In: Rickenmann, D., Chen, C.-L. (Eds.), Debris Flow Hazards Mitigation. Millpress, Rotterdam, pp. 127–137.
Jomelli, V., Pech, P., Chochillon, C., Brunstein, D., 2004. Geomorphic variations of debris flows and recent climatic change in the French Alps. Clim. Chang. 64, 77–102.
Jomelli, V., Brunstein, D., Grancher, D., Pech, P., 2007. Is the response of hill slope debris flows to recent climate change univocal? A case study in the Massif des Ecrins (French Alps). Climate Change 85, 119–137.
Jomelli, V., Brunstein, D., Vrac, M., Déqué, M., Grancher, D., 2009. Impacts of future climatic change (2070–2099) on the potential occurrence of debris flows: a case study in the Massif des Ecrins (French Alps). Clim. Chang. 97, 171–191.
Jomelli, V., Pavlova, I., Utasse, M., Chener, M., Grancher, D., Brunstein, D., Leone, F., 2011. In: Blanco, J.A., Kheradmand, H. (Eds.), Are debris floods and debris avalanches responding univocally to recent climatic change: a case study in the French Alps. InTech, Rijeka, pp. 423–444.
Jonasson, C., 1993. Holocene debris-flow activity in northern Sweden. In: Frenzel, B., Matthews, J.A., Gläser, B. (Eds.), Solifluction and Climate Variations in the Holocene. Paläoklimaforschung, vol. 11. Gustav Fischer Verlag, Stuttgart, pp. 179–195.
Lopez Saez, J., Corona, C., Stoffel, M., Gotteland, A., Berger, F., Liebault, F., 2011. Debris-flow activity in abandoned channels of the Manival torrent reconstructed with LiDAR and tree-ring data. Nat. Hazards Earth Syst. Sci. 11, 1247–1257.
Loye, A., Jaboyedoff, M., Pedrazzini, A., Theule, J., Liebault, F., Metzger, R., 2011. Morphostructural analysis of an alpine debris flow catchment: implication for debris supply. In: Genevois, R., Hamilton, D.L., Prestininzi, A. (Eds.), Proceedings 5th International Conference on Debris-Flow Hazards Mitigation. La Sapienza, Rome, pp. 215–226.
Magliulo, P., Di Lisio, A., Russo, F., Zelano, A., 2008. Geomorphology and landslide susceptibility assessment using GIS and bivariate statistics: a case study in southern Italy. Nat. Hazards 47, 411–435.
Marchi, L., Cavalli, M., 2007. Procedures for the documentation of historical debris flows: application to the Chieppena Torrent (Italian Alps). J. Environ. Manag. 40, 493–503.
Matthews, J.A., Dahl, S.O., Dresser, P.Q., Berrisford, M.S., Lie, O., Nesje, A., Owen, G., 2009. Radiocarbon chronology of Holocene colluvial (debris-flow) events at Sletthamn, Jotunheimen, southern Norway: a window on the changing frequency of extreme climatic events and their landscape impact. The Holocene 19, 1107–1129.
Météo-France, 2011. Etude du changement climatique pour le SRCAE Rhône-Alpes; Météo-France — Direction Inter-Régionale Centre Est (73 pp.).
Meyzenq, C., 1984. Hautes-Alpes, Ubaye, Hauy-Drac, Prealpes Dromoises. Pays de transition entre Alpes du Nord et Alpes du Sud. Edition Ophrys (954 pp.).
ONERC, 2008. Changements climatiques dans les Alpes: Impacts et risques naturels. Rapport Technique de l'ONERC (98 pp.).
Pavlova, I., Jomelli, V., Brunstein, D., Grancher, D., Vrac, M., 2011. Debris flow occurrence and meteorological factors in the French Alps: a regional investigation. In: Genevois, R., Hamilton, D.L., Prestininzi, A. (Eds.), Proceedings 5th International Conference on Debris-Flow Hazards Mitigation. La Sapienza, Rome, pp. 127–135.
Pelfini, M., Santilli, M., 2008. Frequency of debris flows and their relation with precipitation: a case study in the Central Alps, Italy. Geomorphology 101, 721–730.
Piazza, M., Page, C., Sanchez, E., Terray, L., 2011. Comparaison des méthodes de désagrégation statistique et dynamique pour l'évaluation du changement climatique sur les zones de montagnes en France. SCAMPEI Rapport semestriel d'activité (28 pp.).
Plaut, G., Simonnet, E., 2001. Large-scale circulation classification, weather regimes, and local climate over France, the Alps and Western Europe. Clim. Res. 17, 303–324.
Quintana-Segui, P., Le Moigne, P., Durand, Y., Martin, E., Habets, F., Baillon, M., Canellas, C., Franchisteguy, L., Morel, S., 2008. Analysis of near surface atmospheric variables: validation of the SAFRAN analysis over France. J. Appl. Meteorol. Climatol. 47, 92–107.
Rickenmann, D., 1999. Empirical relationships for debris flows. Nat. Hazards 19, 47–77.
Salameh, T., 2008. Modelisation multi-echelles de la circulation atmospherique hivernale sur le bassin Mediterraneen: role des interactions d'echelles (PhD thesis, 144 pp.).
Seynova, I., Sidorova, T., Chernomorets, S., 2007. Debris flow formation processes and dynamics of glaciers in the Central Caucasus. In: Chen, C.-L., Major, J. (Eds.), Debris-Flow Hazards Mitigation: Mechanics, Prediction, and Assessment. Millpress, Rotterdam, pp. 77–86.
Stoffel, M., 2010. Magnitude–frequency relationships of debris flows. A case study based on field surveys and tree-ring records. Geomorphology 116, 67–76.
Stoffel, M., Beniston, M., 2006. On the incidence of debris flows from the early Little Ice Age to a future greenhouse climate: a case study from the Swiss Alps. Geophys. Res. Lett. 33, L16404. http://dx.doi.org/10.1029/2006GL026805.
Stoffel, M., Lievre, I., Conus, D., Grichting, M.A., Raetzo, H., Gartner, H.W., Monbaron, M., 2005. 400 years of debris-flow activity and triggering weather conditions: Ritigraben, Valais, Switzerland. Arct. Antarct. Alp. Res. 37, 387–395.
Stoffel, M., Conus, D., Grichting, M.A., Lievre, I., Maitre, G., 2008. Unraveling the patterns of late Holocene debris-flow activity on a cone in the Swiss Alps: chronology, environment and implications for the future. Glob. Planet. Chang. 60, 222–234.
Theule, J.I., Liebault, F., Loye, A., Laigle, D., Jaboyedoff, M., 2012. Sediment budget monitoring of debris-flow and bedload transport in the Manival Torrent, SE France. Nat. Hazards Earth Syst. Sci. 12, 731–749.
Tropeano, D., Turconi, L., 2004. Using historical documents for landslide, debris flow and stream flood prevention. Nat. Hazards 31, 663–679.
Van Steijn, H., 1996. Debris flow magnitude–frequency relationships for mountainous regions of central and Northwest Europe. Geomorphology 15, 259–273.
Veyrat-Charvillon, S., Menier, M., 2006. Stereophotogrammetry of archive data and topographic approaches to debris-flow torrent measurements: calculation of channel-sediment states and a partial sediment budget for Manival torrent (Isère, France). Earth Surf. Process. Landf. 31, 201–219.
Vidal, J.-P., Martin, E., Franchistéguy, L., Baillon, M., Soubeyroux, J.-M., 2010. A 50-year high-resolution atmospheric reanalysis over France with the Safran system. Int. J. Climatol. 30, 1627–1644.
Wieczorek, G.F., 1987. Effect of rainfall intensity and duration on debris flows in central Santa Cruz Mountains. In: Costa, J.E., Wieczorek, G.F. (Eds.), Debris Flow/avalanches: Process, Recognition, and Mitigation. Geological Society of America. Reviews in Engineering Geology, 7, pp. 93–104.
Wilson, R.C., 1997b. Operation of a landslide warning system during the California storm sequence of January and February 1993. In: Larson, R.A., Slosson, J.E. (Eds.), Storm-induced Geologic Hazards: Case Histories from the 1992–1993 Winter in Southern California and Arizona. Geological Society of America. Reviews in Engineering Geology, 11, pp. 61–70.
Wilson, R.C., 1997a. Normalizing rainfall/debris-flow thresholds along the U. S. Pacific coast for long-term variations in precipitation climate. In: Chen, C.L. (Ed.), Proceedings 1st International Conference on Debris-Flow Hazard Mitigation. American Society of Civil Engineers, San Francisco, pp. 32–43.
Winchester, V., Harrison, S., 1994. A development of the lichenometric method applied to the dating of glacially influenced debris flows in Southern Chile. Earth Surf. Process. Landf. 19, 137–151.
Zhang, J., Shen, X., 2011. The characteristics of genesis and evolution of debris flow based on fixed point observation. In: Genevois, R., Hamilton, D.L., Prestininzi, A. (Eds.), Proceedings 5th International Conference on Debris-Flow Hazards Mitigation. La Sapienza, Rome, pp. 283–291.
Zimmermann, M., 1990. Debris flows 1987 in Switzerland: geomorphological and meteorological aspects proceedings of two Lausanne Symposium. IAHS Publ. 194 (387-393).
Zischg, A., Curtaz, M., Galuppo, A., Lang, K., Mayr, V., Riedl, C., Schoeneich, P., 2011. Chapter 2: Permafrost and debris-flows. In: Schoeneich, P., et al. (Eds.), Hazards Related to Permafrost and to Permafrost Degradation. PermaNET Project, State-of-the-art Report, 6.2. On-line Publication. ISBN: 978-2-903095-59-8, pp. 29–66.